J. Phys. B: At. Mol. Opt. Phys. **45** (2012) 015205 (6pp) doi:10.1088/0953-4075/45/1/015205

The correlated two-centre double continuum and the double ionization of H_2 and N_2 by fast electron impact

O Chuluunbaatar[1], A A Gusev[1] and B B Joulakian[2]

[1] Joint Institute for Nuclear Research, Dubna, Moscow Region 141980, Russia
[2] Université Paul Verlaine-Metz, Laboratoire de Physique Moléculaire et des Collisions, Institut Jean Barriol (FR CNRS 2843), 1 bld Arago, 57078 Metz Cedex 3, France

E-mail: joulak@univ-metz.fr

Received 26 September 2011, in final form 27 October 2011
Published 15 December 2011
Online at stacks.iop.org/JPhysB/45/015205

Abstract
A correlated product of two two-centre continuum Coulomb waves is constructed to describe the state of two ejected electrons in the (e, 3e) double ionization of the two most common and naturally existing diatomic molecules, H_2 and N_2, for which experiments are currently in progress. New computational approaches are introduced to overcome and improve the numerical precision of the calculations involved. We show that the introduction of correlation significantly modifies the outcome of the results.

(Some figures in this article are in colour only in the electronic version)

1. Introduction

The double (e, 3e) ionization designates complete experiments in which an atomic or molecular target is doubly ionized by the impact of an incident electron ejecting two electrons, which are detected in coincidence with the scattered electron [1]. These experiments give precious insight into the electronic structure of the targets, help to verify the different hypothesis about the possible ionization mechanisms and above all they represent, with the photo-double ionization, experimental means to quantify electron–electron correlation, which is the main cause of the double ionization of bound electrons by a single electron or photon. Double ionization, in general, can also be considered as a process in which an important amount of energy is deposited in the target. This can be, in the case of the ionization of organic molecules, the main cause of cellular death. Monte Carlo calculations nowadays are undertaken to determine the effects of collisions of the secondary electrons produced in the irradiation of living matter by heavy ions [2] which cause major damage by ionizing the molecules of living matter.

In the case of atoms, and particularly in the case of helium, it has been shown [3] that correlated 3C functions are necessary to obtain satisfactory results when used to describe the two ejected electrons in the photo-double ionization (γ, 2e) of helium. Similar applications of the (e, 3e) ionization of helium [4, 5] have also shown the importance of correlation by introducing the same 3C correlated function. In the case of the double ionization of diatomic molecules, the correlated product of two two-centre mono-electronic wavefunctions developed in [6, 7] has been successfully applied to the photo-double ionization (γ, 2e) of H_2 [8].

In this paper, we determine the multi-fold differential cross section of the double (e, 3e) ionization of H_2 and the outermost electrons of N_2 by using the correlated two-centre continuum (TCC) wave for the description of the ejected electrons in a procedure, which takes into account only the first term of the Born series. We apply new computational approaches both in the numerical integration and the calculation of the confluent hypergeometric functions. Our aim is first of all to interact with the actual experimental efforts to produce data for the (e, 3e) double ionization of N_2 and compare our results obtained by the present correlated function for the (e, 3–1e) ionization of H_2 to the experimental results [9] and to those obtained by the uncorrelated function [10], by the external complex scaling method [11] and by the second Born treatment [12].

2. Theory

The multiply differential cross section (MDCS) of a general out-of-plane detection of the scattered and the two ejected

electrons from a diatomic molecule is sixfold, and is given by

$$\sigma^{(6)} = \frac{\mathrm{d}^6\sigma}{\mathrm{d}\Omega_\rho\,\mathrm{d}\Omega_s\,\mathrm{d}\Omega_1\,\mathrm{d}\Omega_2 d\left(k_1^2/2\right)d\left(k_2^2/2\right)} = \frac{k_s k_1 k_2}{k_i}|T_{fi}|^2, \tag{1}$$

where $\mathrm{d}\Omega_s$, $\mathrm{d}\Omega_1$, $\mathrm{d}\Omega_2$ and $\mathrm{d}\Omega_\rho$, are respectively the elements of the solid angles for the orientations of the scattered and the ejected electrons and the internuclear axis $\boldsymbol{\rho}$. k_i, k_s, k_1 and k_2 represent respectively the moduli of the wave vectors of the incident, scattered and ejected electrons. In the case of randomly oriented targets, we must pass to the fivefold differential cross section (FDCS) by integrating overall possible and equally probable directions of the molecule in space

$$\sigma^{(5)} = \frac{1}{4\pi}\int \mathrm{d}\Omega_\rho \sigma^{(6)}(\rho). \tag{2}$$

The conservation of the energy for the fixed internuclear distance ρ gives

$$E_i = E_s + E_1 + E_2 + I, \tag{3}$$

where E_i, E_s, E_1 and E_2 represent respectively the energies of the incident, scattered and ejected electrons, with I being the energy necessary to eject two electrons from the target at the equilibrium internuclear distance. We define the transition matrix element by the first term of the Born series:

$$T_{fi} = \frac{1}{2\pi}\int \mathbf{dr}_0 \int \mathbf{dr}_1 \times \int \mathbf{dr}_2 \exp(\imath \mathbf{K}\mathbf{r}_0)\bar{\chi}_f(\mathbf{r}_1,\mathbf{r}_2)V\varphi_i(\mathbf{r}_1,\mathbf{r}_2). \tag{4}$$

Here, the overline indicates the complex conjugate. $\mathbf{r}_0$ is the position of the fast incident–scattered electron, which we will describe as a plane wave. $\mathbf{r}_j$ $(j = 1, 2)$ refer to the positions of the bound (ejected) electrons. $\mathbf{K} = \mathbf{k}_i - \mathbf{k}_s$ is the momentum transferred to the target and V represents the Coulomb interaction between the incident electron and the target given by

$$V = -\frac{1}{|\mathbf{r}_0 - \boldsymbol{\rho}/2|} - \frac{1}{|\mathbf{r}_0 + \boldsymbol{\rho}/2|} + \frac{1}{|\mathbf{r}_0 - \mathbf{r}_1|} + \frac{1}{|\mathbf{r}_0 - \mathbf{r}_2|}. \tag{5}$$

Integrating over the position of the fast incident electron $\mathbf{r}_0$ using the Bethe transformation, we have

$$T_{fi} = \frac{2}{K^2}\int \mathbf{dr}_1 \int \mathbf{dr}_2 \exp(\imath \mathbf{K}\mathbf{r}_0)\bar{\chi}_f(\mathbf{r}_1,\mathbf{r}_2) \times (-2\cos(\mathbf{K}\boldsymbol{\rho}/2) + \exp(\imath \mathbf{K}\mathbf{r}_1) + \exp(\imath \mathbf{K}\mathbf{r}_2))\varphi_i(\mathbf{r}_1,\mathbf{r}_2). \tag{6}$$

The final state wavefunction

$$\chi_f(\mathbf{r}_1,\mathbf{r}_2) = \frac{\phi_f(\mathbf{k}_1,\mathbf{r}_1,\mathbf{k}_2,\mathbf{r}_2) + \phi_f(\mathbf{k}_1,\mathbf{r}_2,\mathbf{k}_2,\mathbf{r}_1)}{\sqrt{2}} \tag{7}$$

describes the state of the two equivalent ejected electrons, where

$$\phi_f(\mathbf{k}_1,\mathbf{r}_1,\mathbf{k}_2,\mathbf{r}_2) = v(k_{12})\,{}_1F_1(\imath\alpha_{12},1, -\imath(k_{12}r_{12} + \mathbf{k}_{12}\mathbf{r}_{12}))T(\mathbf{k}_1,\mathbf{r}_1)T(\mathbf{k}_2,\mathbf{r}_2), \tag{8}$$

in which, we have introduced, as in the case of atoms [4] the electron–electron correlation. Here, $\mathbf{r}_{12} = \mathbf{r}_1 - \mathbf{r}_2$ and

$$v(k_{12}) = \exp\left(-\frac{\pi\alpha_{12}}{2}\right)\Gamma(1 - \imath\alpha_{12}) \tag{9}$$

represents the Gamow factor with

$$\alpha_{12} = \frac{1}{2k_{12}}, \qquad \mathbf{k}_{12} = \frac{1}{2}(\mathbf{k}_1 - \mathbf{k}_2). \tag{10}$$

The final state wavefunction satisfies the orthonormality condition in the sense

$$\langle\phi_f(\mathbf{k}_1,\mathbf{r}_1,\mathbf{k}_2,\mathbf{r}_2)|\phi_f(\mathbf{k}_1',\mathbf{r}_1,\mathbf{k}_2',\mathbf{r}_2)\rangle = \delta(\mathbf{k}_1 - \mathbf{k}_1')\delta(\mathbf{k}_2 - \mathbf{k}_2'). \tag{11}$$

The TCC wavefunction

$$T(\mathbf{k}_i,\mathbf{r}_j) = \exp(-\pi\alpha_i)(\Gamma(1-\imath\alpha_i))^2\frac{\exp(\imath\mathbf{k}_i\mathbf{r}_j)}{(2\pi)^{3/2}} \times {}_1F_1(\imath\alpha_i,1,-\imath(k_i r_{ja} + \mathbf{k}_i\mathbf{r}_{ja}))\,{}_1F_1 \times (\imath\alpha_i,1,-\imath(k_i r_{jb} + \mathbf{k}_i\mathbf{r}_{jb})) \tag{12}$$

is borrowed from [10]. It describes the ejected electron in the field of two Coulomb centres with

$$\alpha_i = -\frac{Z_i}{k_i}, \quad \mathbf{r}_{ja} = \mathbf{r}_j + \boldsymbol{\rho}/2, \quad \mathbf{r}_{jb} = \mathbf{r}_j - \boldsymbol{\rho}/2, \quad i, j = 1, 2, \tag{13}$$

and $Z_i = 1$. Finally, $\varphi_i(\mathbf{r}_1,\mathbf{r}_2)$ represents the space part of the initial state wavefunction.

Taking into account the symmetry of the final and initial functions $\varphi_i(\mathbf{r}_1,\mathbf{r}_2) = \varphi_i(\mathbf{r}_2,\mathbf{r}_1)$ with respect to the exchange of $\mathbf{r}_1$ and $\mathbf{r}_2$, we can reduce the expression of the transition matrix element to the following six-dimensional integral:

$$T_{fi} = \frac{2\sqrt{2}}{K^2}\int \mathbf{dr}_1 \int \mathbf{dr}_2 \bar{\phi}_f(\mathbf{r}_1,\mathbf{r}_2) \times (-2\cos(\mathbf{K}\boldsymbol{\rho}/2) + \exp(\imath\mathbf{K}\mathbf{r}_1) + \exp(\imath\mathbf{K}\mathbf{r}_2))\varphi_i(\mathbf{r}_1,\mathbf{r}_2). \tag{14}$$

The space coordinates of the wavefunctions are defined in the molecular frame of reference, whose origin is fixed on the centre of mass of the molecule and whose z-axis is parallel to the internuclear vector $\boldsymbol{\rho}$ of constant modulus.

In the case of N_2, for which the equilibrium position $\rho_e = 2.0675$ au, the initial wavefunction describing the valence electrons is given by

$$\varphi_i(\mathbf{r}_1,\mathbf{r}_2) = 3\sigma_g(\mathbf{r}_1)3\sigma_g(\mathbf{r}_2), \tag{15}$$

which is borrowed from [13].

In the case of H_2, we consider the wavefunction $\varphi_i(\mathbf{r}_1,\mathbf{r}_2)$ for the initial electronic Σ_g fundamental state obtained by a variational 14-parameters calculation [14]

$$\varphi_i(\mathbf{r}_1,\mathbf{r}_2) = A_1\psi_1 + A_2\psi_2 + A_3\psi_3, \tag{16}$$

with

$$\begin{aligned}
\psi_1 &= (1 + P_{12})(1 + P_{ab})\exp(-\alpha_1 r_{1a} - \alpha_2 r_{1b} - \alpha_3 r_{2a} - \alpha_4 r_{2b} - \gamma_1 r_{12}),\\
\psi_2 &= (1 + P_{12})\exp(-\alpha_5 r_{1a} - \alpha_6 r_{1b} - \alpha_6 r_{2a} - \alpha_5 r_{2b} - \gamma_2 r_{12}),\\
\psi_3 &= (1 + P_{12})\exp(-\alpha_7 r_{1a} - \alpha_7 r_{1b} - \alpha_8 r_{2a} - \alpha_8 r_{2b} - \gamma_3 r_{12}).
\end{aligned} \tag{17}$$

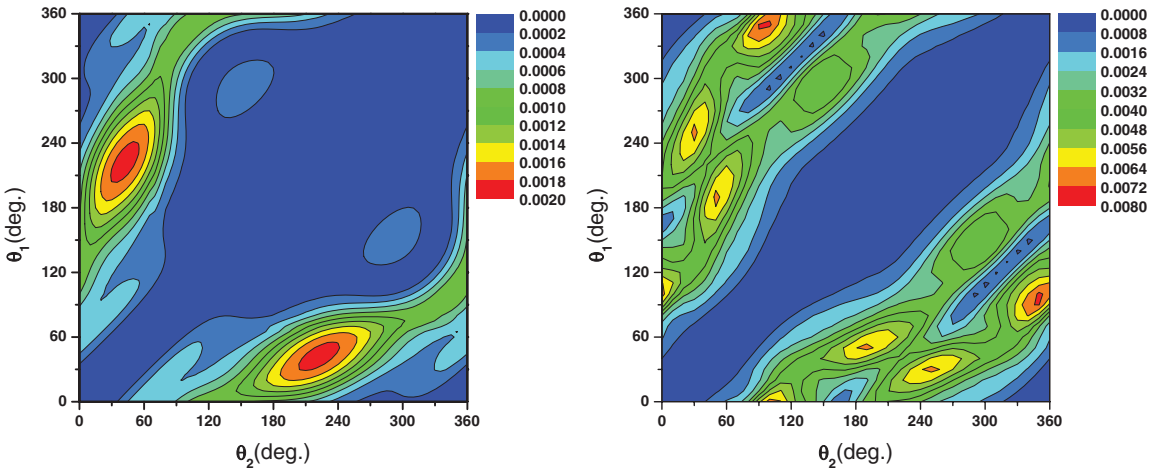

Figure 1. The variation of the FDCS (in au) of the (e, 3e) ionization of N_2 in terms of the two ejection angles θ_1 and θ_2, for $E_i = 617$ eV, $E_s = 500$ eV, $E_1 = E_2 = 37$ eV and $\theta_s = -6^\circ$. (a) Without ${}_1F_1(\imath\alpha_{12}, 1, -\imath(k_{12}r_{12} + \mathbf{k}_{12}\mathbf{r}_{12}))$. (b) With ${}_1F_1(\imath\alpha_{12}, 1, -\imath(k_{12}r_{12} + \mathbf{k}_{12}\mathbf{r}_{12}))$.

Here, P_{12} and P_{ab} are the operators that interchange electrons ($1 \longleftrightarrow 2$) and the two nuclei ($a \longleftrightarrow b$), respectively.

For both molecules the correlated TCC product, described above, was used with the total charge $Z = Z_1 + Z_2 = 2$ to satisfy the asymptotic conditions of the doubly charged residual ions. The FDCS for both molecules will be obtained by six-dimensional integrals, whose numerical calculations were optimized by the application of an original and practical method of determination of the confluent hypergeometric functions presented in the appendix and the adoption of a very efficient numerical integration procedure.

It is evident that, when we neglect, as a first step, the correlation in the final state wavefunction $\phi_f(\mathbf{r}_1, \mathbf{r}_2)$ represented by the confluent hypergeometric function ${}_1F_1(\imath\alpha_{12}, 1, -\imath(k_{12}r_{12} + \mathbf{k}_{12}\mathbf{r}_{12}))$, the transition matrix element of N_2 will be given by the products of two three-dimensional integrals

$$T_{fi} = \frac{2\sqrt{2}}{K^2} v(k_{12})(-2A_1A_2\cos(\mathbf{K}\boldsymbol{\rho}/2) + A_3A_2 + A_4A_1),$$

$$A_j = \int \mathbf{dr}_j \bar{T}(\mathbf{k}_j, \mathbf{r}_j) 3\sigma_g(\mathbf{r}_j), \quad j = 1, 2,$$

$$A_{2+j} = \int \mathbf{dr}_j \bar{T}(\mathbf{k}_j, \mathbf{r}_j) \exp(\imath\mathbf{K}\mathbf{r}_j) 3\sigma_g(\mathbf{r}_j). \tag{18}$$

In our results, we will present two types of calculations, one, designated by type (a), where we neglect the function ${}_1F_1(\imath\alpha_{12}, 1, -\imath(k_{12}r_{12} + \mathbf{k}_{12}\mathbf{r}_{12}))$ in $\phi_f(\mathbf{k}_1, \mathbf{r}_1, \mathbf{k}_2, \mathbf{r}_2)$ but keep the Gamow factor in equation (9) and the other, without neglecting, designated by type (b). In type (a), the orthogonality of the final state function is conserved but the norm is destroyed (equation (11)) because of the presence of the Gamow factor, and thus the results corresponding to type (a) cannot be considered as absolute in contrast to those of type (b).

3. Results

We have chosen in our calculations the same experimental conditions for both molecules H_2 and N_2. Here, the scattered electron of 500 eV is detected at an angle $\theta_s = -6^\circ$ with respect to the incident electron beam. The ejected electrons of much lower energy values are detected in coincidence with the scattered electron. The energy of the incident electron is chosen by the energy conservation equation (3). In contrast to the double ionization of H_2 for which experimental results are given in [9], no results are available at present for the double ionization of N_2.

In figures 1 and 2, we present plots of the variation of the FDCS of the double ionization of the valence electrons of N_2 for two particular values. $E_1 = E_2 = 37$ eV in figure 1 and $E_1 = E_2 = 12$ eV in figure 2. We can verify first that, as both ejected electrons have the same energy, the symmetry with respect to exchange $\sigma^{(5)}(\theta_1, \theta_2) = \sigma^{(5)}(\theta_2, \theta_1)$ is respected, as the diagonal line $\theta_1 = \theta_2$ is, in all cases, a line of symmetry. We also observe that the regions on the plots which correspond to nearly parallel ejection of the two electrons give very small FDCS values, which is physically reasonable because of Coulomb repulsion. These regions are found in the central band $\theta_1 \approx \theta_2$, and on the two extreme sides $0^\circ < \theta_1 < 60^\circ$, $300^\circ < \theta_2 < 360^\circ$, $300^\circ < \theta_1 < 360^\circ$ and $0^\circ < \theta_2 < 60^\circ$ as expected. This is ensured by the presence of the Gamow factor in equation (9), which is present in both types of calculations (a and b) with and without the final state correlation. In each figure, the color scale (or grey scale) has been chosen in such a way as to ensure the best visibility. Now, as mentioned above, the normalization of the final state wavefunction being destroyed by the presence of the Gamow factor in type (a) but not in type (b) means the comparison between figures 2(a) and (b) can only be qualitative.

The band of interest for the experimentalist is that found between the two lines defined by $\theta_2 = \theta_1 + 60^\circ$ and $\theta_2 = \theta_1 + 300^\circ$. In the correlated cases (figures 1(b) and 2(b)), we

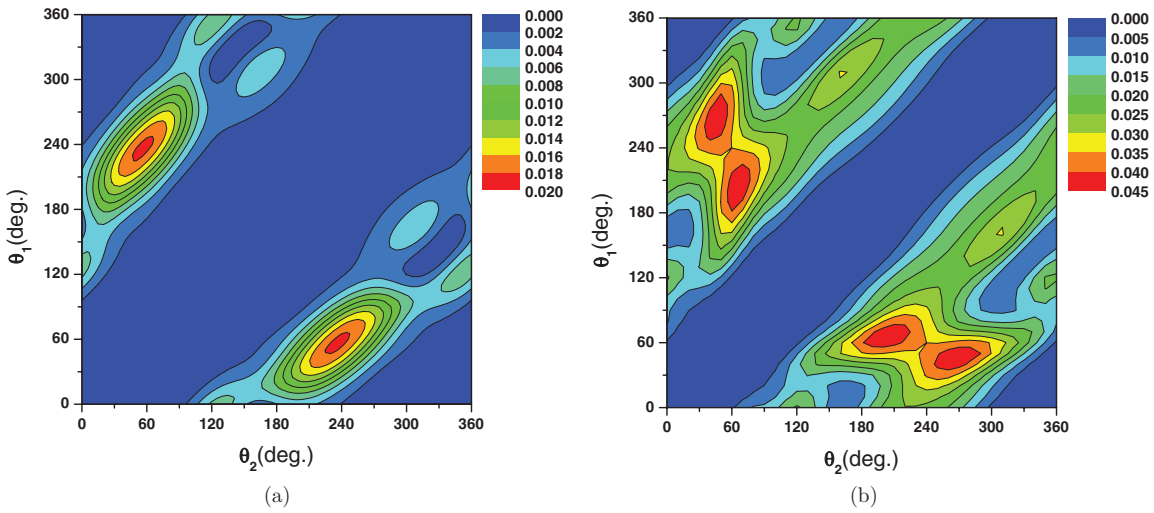

Figure 2. The same as in figure 1 at $E_i = 567$ eV, $E_s = 500$ eV and $E_1 = E_2 = 12$ eV.

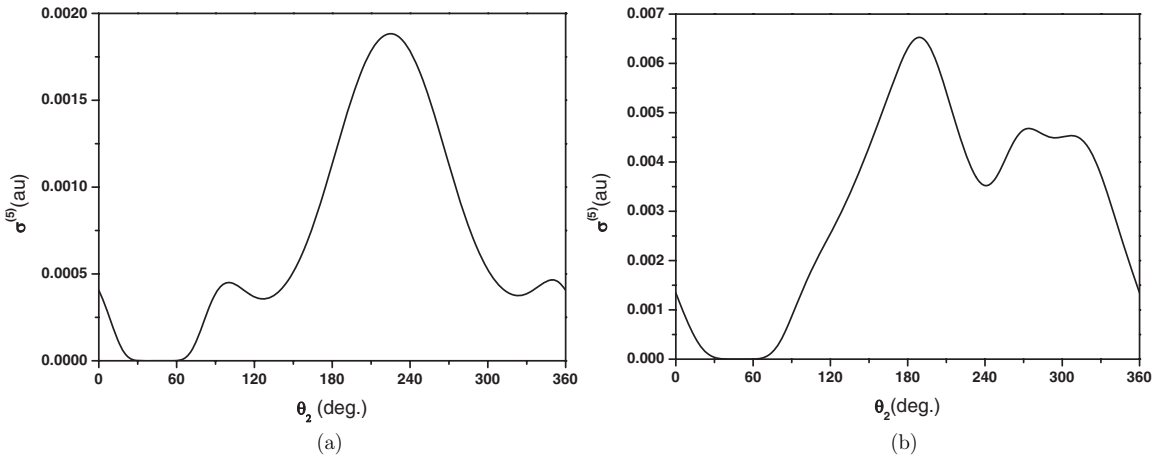

Figure 3. The variation of the FDCS of the (e, 3e) ionization of N_2 in terms of the ejection angle θ_2 for the same energy values as in figure 1, $\theta_1 = 45^\circ$ and $\theta_s = -6^\circ$.

observe a 'valley' along the direction $\theta_2 \approx \theta_1 + 180^\circ$. This valley has already been observed in the case of the photo-double ionization of atoms such as He and Be in [15] and that of (e, 3e) calculations of He [5, 16] and for Be in [17]. This valley is only partially present in the non-correlated cases (figures 1(a) and 2(a)), which is interrupted by the peaks around $\theta_1 \approx 40^\circ$ and $\theta_2 \approx 220^\circ$ in figure 1(a) and around $\theta_1 \approx 50^\circ$ and $\theta_2 \approx 240^\circ$ in figure 2(a), which has no physical significance. On the other hand, the valley and thus its neighbouring maxima observed in the same region of figures 1(b) and 2(b) are well explained in the dipole regime by the binary and recoil maxima (see [16]).

To present the above results quantitatively, we consider the variation of the FDCS in terms of one of the ejection directions keeping the other angle fixed. In figures 3(a) and (b) we show this variation for the energy conditions of figure 1 and $\theta_1 = 45^\circ$. In figures 4(a) and (b), we consider the energy conditions of figure 2 and fix $\theta_1 = 60^\circ$. These 2D curves give the magnitude and show clearly the effect of the introduction of the correlation as discussed above.

Let us now pass to the results for the (e, 3–1e) double ionization of H_2, which corresponds to an (e, 3e) experiment [9] in which only one of the ejected electrons is detected in coincidence with the scattered electron. Experimentally, this is interesting, as the number of coincidence events increases significantly, making it easier to reproduce the needed statistics. The energy conservation ensures that the coincidences observed correspond well with a double ionization event. In figure 5, we compare our results obtained by the full correlated function given by the black continuous line to those given by the complex scaling method [11] (broken line) to those obtained by the application of the uncorrelated TCC product [10] (dotted line) and by the application of the simplified second Born method [12] (crossed line). We have scaled these theoretical results to our result at the maximum of around 345°. The experimental results [9] on the other hand were scaled to our results around 300°. We observe that all theoretical approaches reproduce curves, which are symmetrical around 345°, the direction of the momentum transfer $\mathbf{K} = \mathbf{k}_i - \mathbf{k}_s$ which is an axis of symmetry in the first Born theory. The experimental peak is found around 320°, and for the moment, neither theory can reproduce this result. We observe nevertheless that our correlated results in the continuous black line show an improvement, when compared

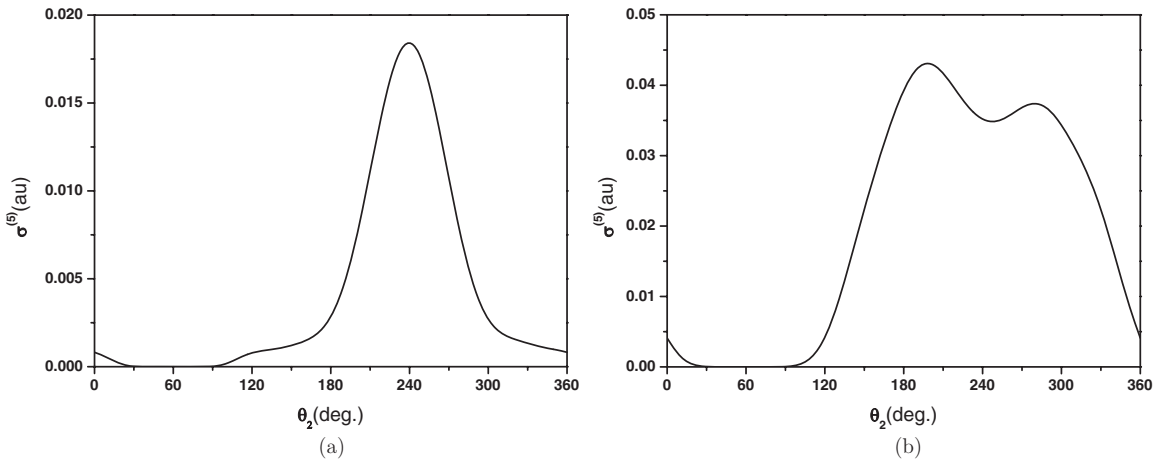

Figure 4. The variation of the FDCS in (au) of the (e, 3e) ionization of N_2 in terms of the ejection angle θ_2 for the same energy values as in figure 2, $\theta_1 = 60^\circ$.

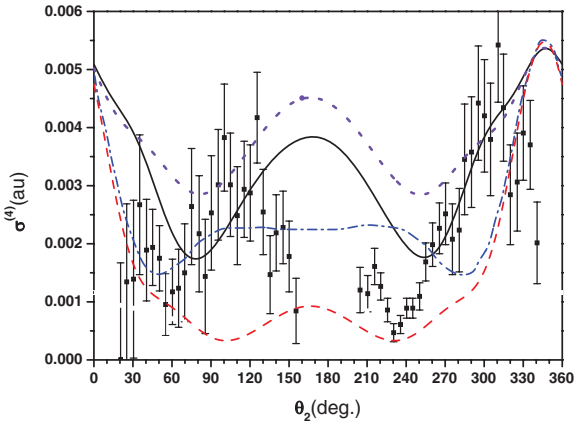

Figure 5. The variation of the fourfold differential cross section of the (e, 3–1e) ionization H_2 for $E_i = 612$ eV, $E_s = 500$ eV, $E_1 = 10$ eV, $E_2 = 51$ eV. $\theta_s = 1.5^\circ$. Present work, continuous line. Full squares with error bars correspond to the experimental results of [9] scaled to the theory for the best visual fit at the binary lobe (around 300°). Dotted line [10], broken line [11], and crossed line [12] are scaled to the continuous line at 345°.

especially with the one corresponding to the uncorrelated TCC (dotted line). It very nearly passes the experimental values in the regions found between 250° and 300° and in the region between 90° and 120°. More experimental results with higher incident electron energy values are needed in the future to tackle the present disagreement with the theory.

4. Conclusion

We have determined fully differential cross sections of the (e, 3e) of the valence electrons of N_2 in an approximation where no account has been taken of the interaction incident electron with the core by employing an appropriate correlated TCC wavefunction for the description of the two slow ejected electrons. We have shown that the introduction of the correlated part of the final state wavefunction is necessary to reproduce the characteristic structure of the (e, 3e) curve observed in the case of other targets. We also observe that the introduction of the final state correlation improves significantly the results on the (e, 3–1e) of H_2.

Acknowledgments

We thank Dr T F Sapojnikova for a useful discussion on computations in parallel. This work was partially supported by the RFBR grant no 11-01-00523 and by the theme 09-6-1060-2005/2013 'Mathematical support of experimental and theoretical studies' conducted by JINR.

Appendix. High performance and rapid algorithm for the calculation of the confluent hypergeometric function

Let us consider the confluent hypergeometric function $y(x) = {}_1F_1(a, b, \imath x)$ with the complex parameters a and b and argument x on the finite interval $x \in [0, x_{\max}]$. This function satisfies Kummer's equation:

$$x\frac{\mathrm{d}^2 y(x)}{\mathrm{d}x^2} + (b - \imath x)\frac{\mathrm{d}y(x)}{\mathrm{d}x} - \imath a y(x) = 0. \qquad \text{(A.1)}$$

High-order derivatives of $y(x)$ are calculated by the relation

$$\frac{\mathrm{d}^n y(x)}{\mathrm{d}x^n} = \imath^n \frac{\Gamma(b)}{\Gamma(a)}\frac{\Gamma(a+n)}{\Gamma(b+n)}\,{}_1F_1(a+n, b+n, \imath x). \qquad \text{(A.2)}$$

Using equation (A.1) we obtain the recurrence formula for the derivatives of $y(x)$:

$$x\frac{\mathrm{d}^n y(x)}{\mathrm{d}x^n} + (b + n - 2 - \imath x)\frac{\mathrm{d}^{n-1} y(x)}{\mathrm{d}x^{n-1}} - \imath(a + n - 2)\frac{\mathrm{d}^{n-2} y(x)}{\mathrm{d}x^{n-2}} = 0, \quad n \geqslant 2. \qquad \text{(A.3)}$$

The main idea of the algorithm is to use the predetermined values of $y(x)$ and their derivatives on the set of points

$\{x_i = h\,i\}_{i=0}^{N}$ with step $h = x_{\max}/N$. For the interval $x \in [0, x_{\max}]$, the Taylor series gives

$$y(x) \approx \bar{y}(x) = y(x_{i_o}) + \sum_{i=1}^{n} \frac{1}{i!} \frac{\mathrm{d}^i y(x)}{\mathrm{d}x^i}\bigg|_{x=x_{i_o}} (x - x_{i_o})^i. \tag{A.4}$$

The optimal point x_{i_o} is defined from the condition $\min_{0\leqslant i\leqslant N} |x - x_i|$. From here we obtain $i_o = [x/h + 1/2]$ and $|x - x_{i_o}| \leqslant h/2$, where $[x]$ designates the integer part of x.

If $h < 1$, the double precision $|y(x) - \bar{y}(x)| \leqslant \epsilon = 2 \times 10^{-16}$ is usually achieved at $n < 20$.

For the beforehand calculated values of $y(x)$ and their derivatives on the set of points $\{x_i\}_{i=0}^{N}$, we use the Fortran code CONHYP [18].

Also if $x_i > 2$, the high-order derivatives of $y(x_i)$ can be obtained from the recurrence formula (A.3), using only numerical values of $y(x_i)$ and its first derivative.

References

[1] Lahmam-Bennani A, Duguet A, Dal Cappello C, Nebdi H and Piraux B 2003 *Phys. Rev.* A **67** 010701

[2] Champion C, Hanssen J and Hervieux P A 2002 *Phys. Rev.* A **65** 022710

[3] Maulbetsch F, Pont M, Briggs J and Shakeshaft H 1995 *J. Phys. B: At. Mol. Opt. Phys.* **28** L341–7

[4] Joulakian B, Dal Cappello C and Brauner M 1992 *J. Phys. B: At. Mol. Opt. Phys.* **25** 2863–72

[5] Joulakian B and Dal Cappello C 1993 *Phys. Rev.* A **47** 3788–95

[6] Joulakian B, Hanssen J, Rivarola R and Motassim A 1996 *Phys. Rev.* A **54** 1473–9

[7] Chuluunbaatar O, Joulakian B B, Puzynin I V, Tsookhuu K H and Vinitsky S I 2004 *J. Phys. B: At. Mol. Opt. Phys.* **37** 2607–16

[8] Walter M and Briggs J 1999 *J. Phys. B: At. Mol. Opt. Phys.* **32** 2487–501

[9] Lahmam-Bennani A, Duguet A and Roussin S 2002 *J. Phys. B: At. Mol. Opt. Phys.* **35** L59–63

[10] Chuluunbaatar O, Joulakian B B, Puzynin I V, Tsookhuu K H and Vinitsky S I 2008 *J. Phys. B: At. Mol. Opt. Phys.* **41** 015204

[11] Serov V V and Joulakian B B 2009 *Phys. Rev.* A **80** 062713

[12] Mansouri A, Dal Cappello C, Houamer S, Charpentier I and Lahmam-Bennani A 2004 *J. Phys. B: At. Mol. Opt. Phys.* **37** 1203–14

[13] Scherr C W 1955 *J. Chem. Phys.* **23** 569–78

[14] Turbiner A V and Guevara N L 2007 pp 1–8 arXiv:physics/0606120v2 [physics.atom-ph]

[15] Kheifets A S and Bray I 2001 *Phys. Rev.* A **65** 012710

[16] Kheifets A S 2004 *Phys. Rev.* A **69** 032712

[17] Becher M, Joulakian B, Le Sech C and Chrysos M 2008 *Phys. Rev.* A **77** 052710

[18] Nardin M, Perger W F and Bhalla A 1992 *ACM Trans. Math. Softw.* **18** 345–9